JGR Oceans

RESEARCH ARTICLE
10.1029/2020JC017017

Key Points:

- A shelf break West Greenland Coastal Current exists about half a year between Cape Farewell and Cape Desolation, with a three current system at the Overturning in the Subpolar North Atlantic Program (OSNAP) West section
- The shelf system is strongest in fall, with largest freshwater transport (25–40 mSv), with a transport minimum in spring (15–25 mSv)
- The transport decreases as water is lost offshore, decreasing from OSNAP East (0.61 Sv) to Cape Desolation (0.41 Sv)

Supporting Information:

Supporting Information may be found in the online version of this article.

Correspondence to:

P. G. Myers,
pmyers@ualberta.ca

Citation:

Gou, R., Feucher, C., Pennelly, C., & Myers, P. G. (2021). Seasonal cycle of the coastal west Greenland current system between Cape Farewell and Cape Desolation from a very high-resolution numerical model. *Journal of Geophysical Research: Oceans*, *126*, e2020JC017017. https://doi.org/10.1029/2020JC017017

Received 25 NOV 2020
Accepted 3 MAY 2021

Seasonal Cycle of the Coastal West Greenland Current System Between Cape Farewell and Cape Desolation From a Very High-Resolution Numerical Model

Ruijian Gou[1,2], Charlène Feucher[2], Clark Pennelly[2], and Paul G. Myers[2]

[1]Key Laboratory of Physical Oceanography and Frontiers Science Center for Deep Ocean Multispheres and Earth System, Ocean University of China, Qingdao, China, [2]Department of Earth and Atmospheric Sciences, University of Alberta, Edmonton, Alberta, Canada

Abstract The shelf based West Greenland Current System carries both Arctic Water and Greenland meltwater around Cape Farewell, the southern tip of Greenland, where it may impact the deep water formation in the Labrador Sea. Nevertheless, this current system remains largely unknown due to limited observations. Using a very high-resolution (1°/60°) numerical simulation integrated from 2005 to 2014, the annual cycle of the current structure in the vicinity of southern Greenland is analyzed to present the seasonal variability of the West Greenland Current System. A distinct shelf break West Greenland Coastal Current (WGCC) exists for about half the year between Cape Farewell and Cape Desolation, although it merges with the main jet of the West Greenland Current (WGC) in winter and separates in summer. The WGC has three components at Juliannehaab Bight: A shelf component, a shelf-break component and a main slope jet. The shelf system is most energetic in fall, when the freshwater transport is also the greatest in a range of 25–40 mSv, with a broad transport minimum in spring in a range of 15–25 mSv. The seasonal cycle is strongest near Cape Farewell and weakest at Cape Desolation. The strength of the shelf system decreases as one moves north as water is lost offshore, with strongest transports of 0.61 Sv to the east of Cape Farewell and weakest of 0.41 Sv at Cape Desolation. This decrease in transport between Cape Farewell and Cape Desolation suggests substantial exchange between WGCC and WGC in this region.

Plain Language Summary A West Greenland Coastal Current (WGCC), located along the west Greenland continental shelf, was previously found to transport cold, fresh water to the Labrador Sea through exchange with the shelf break current, potentially influencing the deep convection that feeds the climate-related Atlantic Meridional Overturning Circulation. Our very high-resolution regional model is the first to successfully simulate the WGCC, which is difficult due to its very narrow nature. It is shown that the part of the WGCC that rounds the southern tip of Greenland merges with shelf break current in winter, and the WGCC remains separate from the shelf break current in summer. The main WGCC consists of persistent flow on the shelf except when it splits into multiple branches at Juliannehaab Bight. The WGCC significantly strengthens in summer and autumn. Its volume and freshwater transports increase from a minimum in spring to a maximum in October and this cycle weakens northward and westward along the shelf. The decrease in the transport suggests substantial exchange of WGCC water with the West Greenland Current.

1. Introduction

The Labrador Sea is a site of deep convection where dense Labrador Sea Water (LSW) is formed in winter by intense atmospheric forcing, feeding the lower limb of the Atlantic Meridional Overturning Circulation (AMOC) (Feucher et al., 2019; Lozier et al., 2017; Schulze-Chretian & Frajka-Williams, 2018). This convection is known to be very sensitive to lateral exchange of freshwater and heat by modulating the stratification and influencing the restratification after the occurrence of convection (Aagaard & Carmack, 1989; Lozier et al., 2017; Myers & Donnelly, 2008; Myers et al., 2009; Straneo, 2006; Weijer et al., 2012). A decrease in LSW formation has been linked to weakening or even collapse of the AMOC (Danabasoglu et al., 2016; Stouffer et al., 2007; Vellinga & Wood, 2002), although recent Overturning in the Subpolar North Atlantic Program (OSNAP) results find instead a stronger link between the AMOC and the eastern basin of the sub-polar gyre, at least on short interannual timescales (Lozier et al., 2019). With accelerated warming at

high latitudes (IPCC, 2013), increasing freshwater runoff from Arctic regions is converging on the Labrador Sea through surrounding coastal currents (Haine et al., 2015; Yang et al., 2016). The continuous convergence of freshwater could lead to a decrease in LSW formation although no decrease has been observed as of yet (e.g., Yashayaev & Loder, 2017). Additional change is observed related to the enhanced input of warm and salty Irminger Water into the Labrador Sea (Myers et al., 2007, Yashayaev & Loder, 2017). Therefore, understanding the characteristics and variability of the coastal current system around Greenland is crucial in exploring the sensitivity of the convective overturning in the Labrador Sea.

Despite that, there is not a complete and quantitative picture of the boundary current circulation of freshwater, especially for the West Greenland Current (WGC) system, on which only a few studies have focused. Observational (e.g., Myers et al., 2009; Rykova et al., 2015; Schmidt & Send, 2007; Straneo, 2006) and modeling (e.g., Myers, 2005; Pennelly & Myers, 2020; Schulze-Chretien & Frajka-Williams, 2018) studies have illustrated that the WGC is the major route for freshwater to enter the interior of the Labrador Sea, as well as a major heat supplier to accelerate restratification of the Labrador Sea after convection. It was previously revealed by data from altimetry and surface drifters that enhanced variability occurs in the region close to the west coast of Greenland, near Cape Desolation (Cuny et al., 2002; Fratantoni 2001; White & Heywood, 1995). This region is where buoyant eddies form and advect both surface freshwater as well as warm, salty Irminger Water at depth, into the interior of the Labrador Sea. Studies have investigated the manner in which the freshwater is transported into the convection interior, linked to both eddies (e.g., Bracco et al., 2008; de Jong et al., 2014; Katsman et al., 2004), as well as Ekman transport (e.g., Luo et al., 2016; Schulze-Chretien & Frajka-Williams, 2018).

Meanwhile, multiple studies have shown the existence of an East Greenland Coastal Current (EGCC) on Greenland's eastern shelf (e.g., Bacon et al., 2002; Sutherland & Pickart, 2008; Wilkinson & Bacon, 2005). Bacon et al. (2014) showed that the EGCC was stronger in winter than in summer, and was forced equally by winds and buoyancy. Harden et al. (2014) showed that the current had significant variability at synoptic timescales. Increasing freshwater content in the winter and spring suggested a key role of Fram Strait export rather than local runoff (Harden et al., 2014). Holliday et al. (2007) proposed that the EGCC merges with the East Greenland Current/Irminger Current close to Cape Farewell, with the merged coastal current and shelf break jet eventually forming the WGC. Amalgamating data from multiple cruises, Rykova et al. (2015) found a single current at the West Greenland shelf break west of Cape Farewell, near Cape Desolation. From 2 years of mooring data (2014–2016) just east of Cape Farewell along the OSNAP East line, Le Bras et al. (2018) found a vigorous and distinct EGCC as a separate current core to the shelf break East Greenland Current (EGC), with strong, winter intensified freshwater transport in the coastal EGCC branch.

The concept of a WGCC was first put forward by Lin et al. (2018) using velocity data collected in the summer of 2014. This work revealed that the EGCC, instead of merging with shelf break current, maintains its identity as it encounters Cape Farewell and bifurcates such that a small branch stays on the inner west Greenland shelf with a main branch accounting for most of the flow diverted to the outer shelf. The WGCC refers to this part of coastal current that is on the west side of Cape Farewell. However, the study of Lin et al. (2018) is based on a single shipboard survey around the southern tip of Greenland in summer of 2014. Using three cruises that same summer, as well as $\delta^{18}O$ data and drifters, Benetti et al. (2019) noted that the freshwater associated with the EGCC was close to the shore east of Cape Farewell, with most of the flow joining the shelf break current as the flow rounded Cape Farewell, leaving a weak near surface remnant on the shelf southwest and west of Cape Farewell.

A recent modeling study employing passive tracer to analyze Greenland freshwater fluxes found a small branch or pathway of Greenland tracer flowing northward along the west coast of Greenland, inshore of the main branch on the continental shelf break (Dukhovskoy et al., 2019). They also indicated, by tracer shelf-basin flux analysis, that exchange across the southwestern Greenland continental shelf break accounts for 85% of the Greenland freshwater anomaly from the shelf to the interior Labrador Sea.

With the latest data from the first high-resolution mooring array deployed across the West Greenland boundary current system, from 2014 to 2018, as part of OSNAP (Lozier et al., 2017), Pacini et al. (2020) observed a WGCC as a separate surface intensified flow in the vicinity of the outer shelf and shelf break,

although it merged with the WGC in the annual mean. They also found the WGCC to have its maximum transport in spring when its waters were the warmest and freshest.

Thus there is still considerable uncertainty in how the EGCC influences the currents to the west of Cape Farewell (Figure 1a). Considering the fact that the coastal current entrains the freshest, most buoyant water from the Arctic as well as Greenland ice sheet discharge, the impact on the occurrence of deep convection could be very significant once freshwater is fluxed into interior Labrador Sea (Lin et al., 2018). The Greenland coastal currents are typically characterized with a width between 15 and 20 km (Bacon et al., 2014). Limited observations outside of summer along with very narrow structure mean that these coastal currents are often poorly resolved in observational studies. We thus use an extremely high-resolution numerical model, run with a mesoscale resolving horizontal resolution of 1°/60° for the Labrador Sea (Pennelly & Myers, 2020). The ability of a model of such a resolution to resolve the Rossby Radius on the shelf is discussed in Section 2.

We use a decade of this model's output, with a spatial resolution of 800–900 m in the vicinity of Cape Farewell, to explore the structure and variability features of the west Greenland coastal current system including the WGC and WGCC.

The study is organized as follows: Section 2 describes the simulation used. Section 3 presents the properties and seasonal variability of the coastal current system in terms of velocity, freshwater content and temperature. Section 4 presents the model transport estimates. Discussion and conclusions are drawn in Section 5.

2. Model Description

The simulation used in this study was implemented with the Nucleus for European Modeling of the Ocean (NEMO; Madec, 2008) numerical framework, version 3.6. The large-scale parent domain was built from the global tripolar ORCA025 mesh and covers the Arctic and the North Hemisphere Atlantic (ANHA; Hu et al., 2018) from Bering Strait to 20°S at ¼° resolution (ANHA4). Two nests are then created using the Adaptive Grid Refinement In Fortran package (AGRIF; Debreu et al., 2008). The first is a 1°/12° nest in the North Atlantic subpolar gyre with a 1°/60° additional inner nest for the Labrador Sea. Except resolution-dependent parameters (e.g., model time step, horizontal viscosity, and diffusivity), all parameters are consistent with the ANHA4 configuration. Two-way feedback is applied to allow communication between the parent domain and the nest along the boundary as well as from the nest interior back onto the parent domain. For both parent and nested domains, the initial (3-D temperature, salinity, horizontal velocities, as well as two-dimensional sea surface height, and sea-ice) and open boundary (ocean temperature, salinity, and velocities) conditions are provided by the Global Ocean Reanalyzes and Simulations (GLORYS1v1) data-set (Ferry et al., 2010). No-slip lateral boundary conditions are used within the 1°/60° nested domain while free-slip conditions are used in the other domains. More detailed setup of the simulation can be found in Pennelly and Myers (2020).

Atmospheric forcing is supplied by the Canadian Meterological Centre's Global Deterministic Prediction System ReForecast product (henceforth CGRF; Smith et al., 2014) and features hourly forcing fields of 10 m wind speed, 2-m temperature and specific humidity, incoming shortwave and longwave radiation, as well as precipitation. CGRF has relatively high spatial resolution in the Labrador Sea (33 km). Interannual monthly river runoff (Dai & Trenberth, 2002; Dai et al., 2009) and Greenland melt water discharge (Bamber et al., 2012) were remapped onto the model grid, with a volume conservation approach, to have a more realistic freshwater input from land to ocean. The runoff data also includes freshwater via Greenland's icebergs, though without an iceberg module, which is presently incompatible with AGRIF, all solid discharge is added to the liquid component. See Marson et al. (2018) for the impact of icebergs as simulated via ANHA4 around Greenland. There is no restoring or surface relaxation applied, leaving the model to evolve freely.

The simulation used in this study was initialized in January 2002 and our analysis ends December 2014. Model output is saved as daily averages of each field for the previous 24 h. The vertical mesh contains 75 geopotential levels from the surface to 5,900 m, with the highest resolution (1 m) at the surface and decreasing vertical resolution with depth (204 m at the bottom); the first 34 levels cover the top 250 m. Partial steps for the model bottom topography are applied (Barnier et al., 2007). Model bathymetry was interpolated from

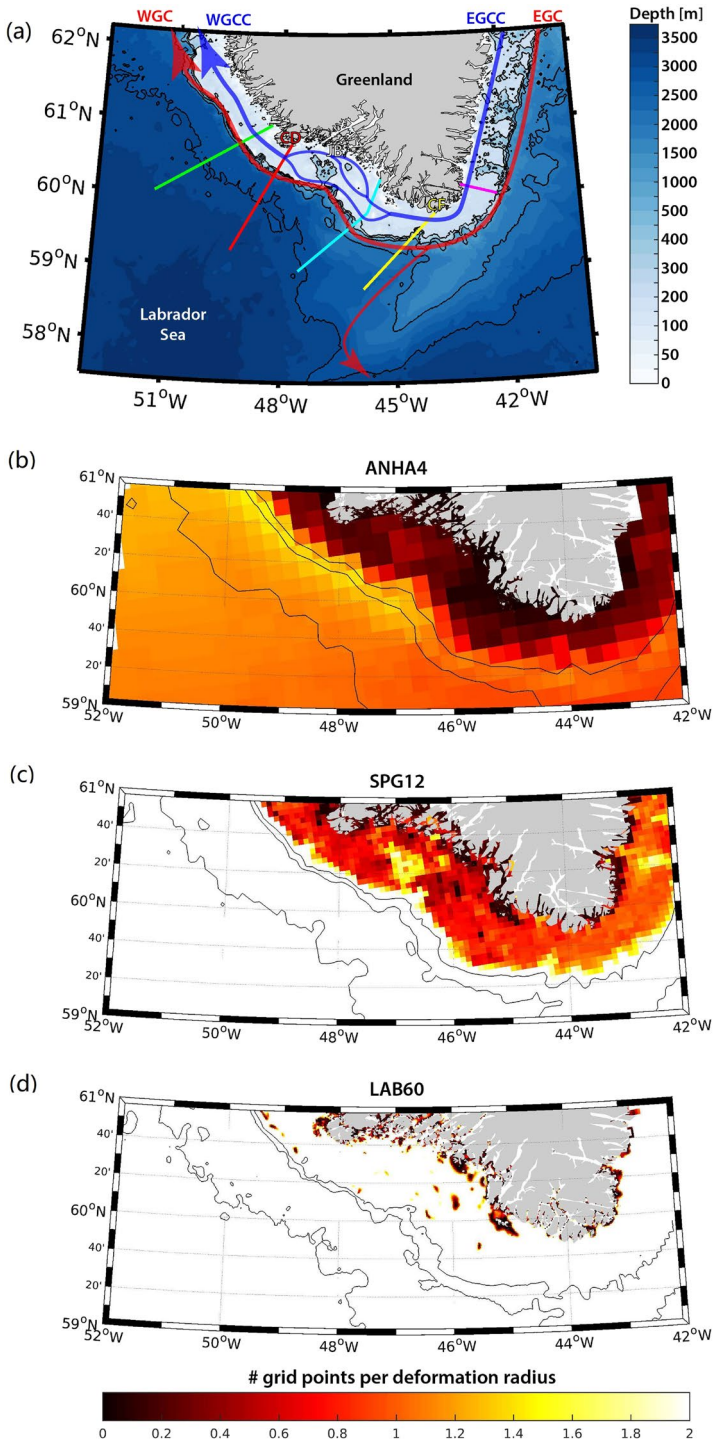

Figure 1. (a) Schematic circulation around the southern tip of Greenland, with the sections marked by the colored lines (Pink—OSNAP East; Yellow—Greenland Institute of Natural Resources (GINR) Cape Farewell standard section; Cyan—OSNAP West; Red—WOCE AR7W line; and Green—GINR Cape Desolation section). The blue and red arrows correspond to the coastal current and shelfbreak current respectively. CF, JB, CD denotes Cape Farewell, Juliannehaab Bight, Cape Desolation respectively. The black contour lines indicate the 250, 500, 1,000, 2,000, and 3,000 m isobaths and the contour interval is non-linear. (b–d) show the number of model grid cells within the first baroclinic deformation radius (averaged over 2005 to 2014) for (b) the parent ¼ degree ANHA4 domain, (c) the intermediate 1°/12° SPG12 nest and (d) the inner 1/60° LAB60 nest. The black contour lines indicate the 1,000, 2,000, and 3,000 m isobaths. The color bar for these 3 panels is located beneath panel (d). OSNAP, Overturning in the Subpolar North Atlantic Program.

the 1°/60° ETOPO GEBCO data-set (Amante & Eakins, 2009) to each domain's grid, though bathymetric smoothing along nest boundaries was carried out in order to conserve volume where the parent domain supplies boundary conditions to the child domain. There may be some uncertainty with the bathymetry close to Cape Farewell, as some topographic features like a seamount just east of OSNAP West do not appear in other bathymetric maps of the region.

The horizontal resolution is around 800–1100 m in the study area of the Labrador Sea, allowing the model to resolve eddies well with a typical radius larger than ~10 km in the Labrador Sea (Lilly et al., 2003). To confirm the need for such resolution, Figure 1d shows it is only within the inner 1°/60° nest (LAB60) that the model resolution allows multiple grid points to resolve the first baroclinic Rossby radius on the shelf, unlike for the parent domain (ANHA4, Figure 1b), as well as the first nest (SPG12, Figure 1c).

3. Results

We begin by looking at the upper ocean (top 50 m) current structure in the vicinity of southern Greenland over the course of the annual cycle (Figure 2). We also consider cross-sections across the current system at the locations of five observational sections (Figures 3 and S1): OSNAP East (Lozier et al., 2017), the Greenland Institute of Natural Resources (GINR) Cape Farewell standard section (Mortensen, 2018), OSNAP West (Lozier et al., 2017), the regularly sampled WOCE AR7W line (Hall et al., 2013) and the GINR Cape Desolation section (Mortensen, 2018). Figure 3 contains model fields for OSNAP East, OSNAP West and Cape Desolation lines, while the model fields for Cape Farewell and AR7W lines are in Figure S1. Note that we extend each section to the coast to capture the inshore processes the model is able to resolve and plot cross-sections seasonally to reduce the number of panels. We define spring, summer, autumn and winter as March–May (MAM), June–August (JJA), September–November (SON) and December–February (DJF), respectively. We average all model fields over 2005–2014 to focus on the long term structure and avoid issues of interannual variability at this stage.

Despite the OSNAP East section just being within the model inner nest, we see a distinct EGCC on the shelf with maximum velocities exceeding 0.3 m s^{-1}, separated by a velocity minimum from the EGC at the shelf break (Figures 2 and 3). That said, a rapid narrowing of the EGCC occurs, as the model current responds to the enhanced resolution and resolved deformation radius (Figure 1d). The deep red band of positive anomalies along the coast shows that the shelf current is widest and has a maximum velocity in winter, with a positive anomaly exceeding 0.1 m s^{-1} in October (Figure 2b). The main current jet, with velocities exceeding 0.5 m s^{-1} through the top 250 m flows around Cape Farewell and continues north along the west Greenland slope past Cape Desolation (Figures 3 and S1). It has a maximum speed in January, decreasing to a minimum in August and September (Figure 2b).

To evaluate the model fields, we compare the time-mean speed and potential density of OSNAP West and OSNAP East lines from August 2014 to April 2016 (Figure S2) to our long term mean model fields (Figure S3). The shelf break current is clearly seen in the observations at the two OSNAP sections just offshore of where the bathymetry drops off below 1,000 m (Figure S2). Here, the shelf current reaches a maximum speed in the upper 50 m of 0.2–0.3 m s^{-1} at OSNAP East and 0.3–0.4 m s^{-1} at OSNAP West. The mean shelf break current in our model (Figure S3) is located similarly, with a velocity core exceeding 0.5 m s^{-1} at the model OSNAP West section. However, the lack of resolution on shelf in the observations makes direct comparison impossible. In both the observations (Figure S2) and model (Figure S3) waters with potential density greater than 27 kg m^{-3} are found below 100 m and 40–50 km offshore at OSNAP East, with waters of similar densities below 100 m and 70 km offshore at OSNAP West. Although we would like to evaluate the model further with direct observations, the lack of observational data on the shelf makes it difficult.

The coastal current remains coherent on the shelf rounding Cape Farewell through to the GINR Cape Farewell line. That said, the current broadens in fall and winter out to the shelf break, while retaining a tight and narrow core in summer with velocities of 0.3–0.4 m s^{-1} separated from the offshore main jet with a region of weak flow slower than 0.1 m s^{-1} (Figures 2 and S4). The broadening is wind driven. To confirm this, we use the JRA55-do reanalysis product (Tsujino et al., 2018) and compute the monthly mean Ekman transports in the region of Cape Farewell (45.3 W-42.3 W, 59.2 N-60.5 N), averaged over 2005–2014. The meridional component of the Ekman transport between OSNAP East and the Cape Farewell line being −0.26 m^2 s^{-1}

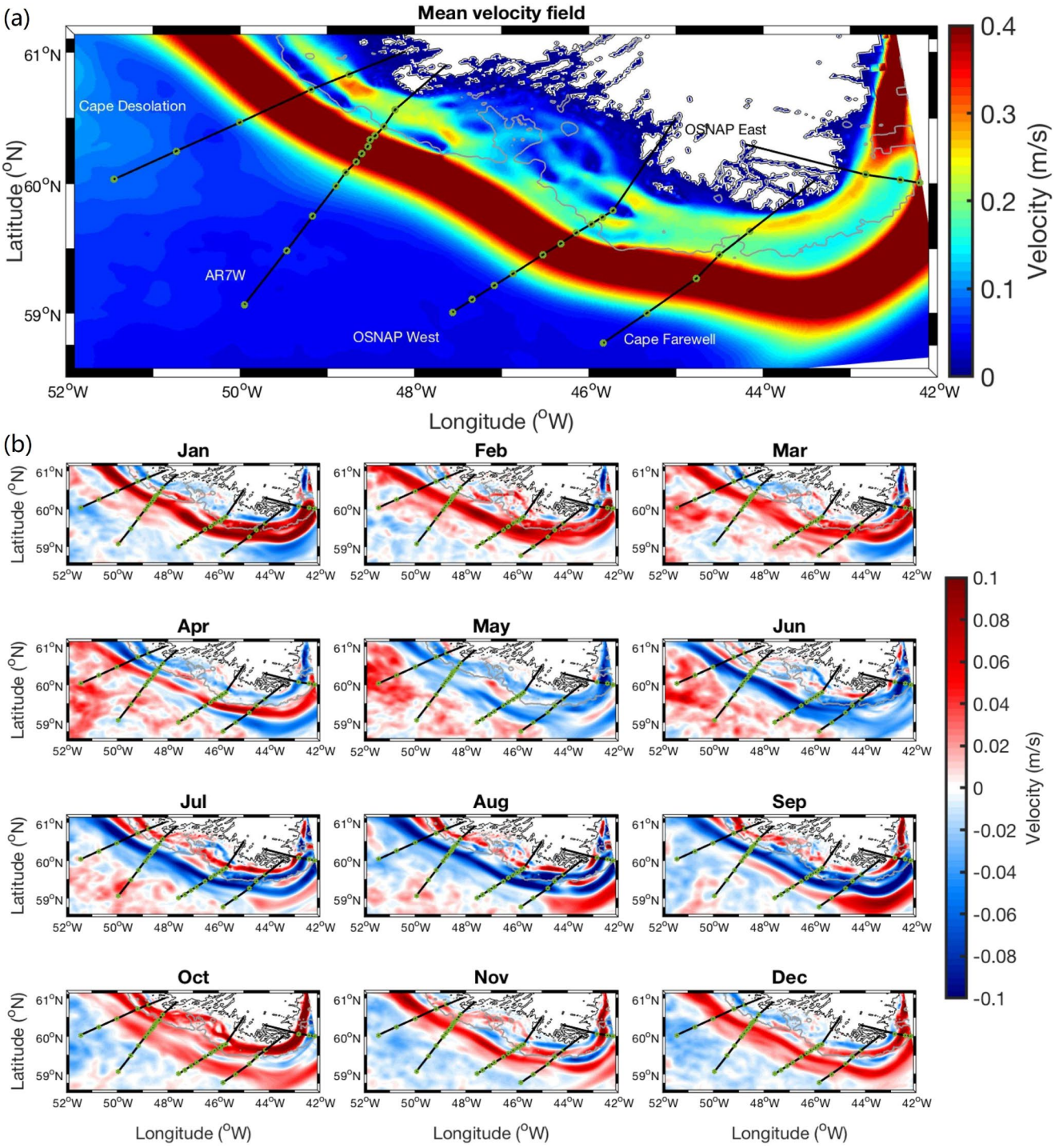

Figure 2. Horizontal maps of the mean top 50 m speed (a) averaged from 2005 to 2014 and the monthly anomalies (b). Sections are shown with green dots representing actual stations and gray lines denote the 250 m isobath.

(southward, offshelf) averaged over November through March compared to 0.05 $m^2\ s^{-1}$ (northward, on-shelf) averaged over May through August. The wintertime acceleration of the current is also related to the winds, with the westward Ekman transport, calculated over the same region as the meridional component, is −0.55 $m^2\ s^{-1}$ over November through March compared to −0.22 $m^2\ s^{-1}$ over May through August.

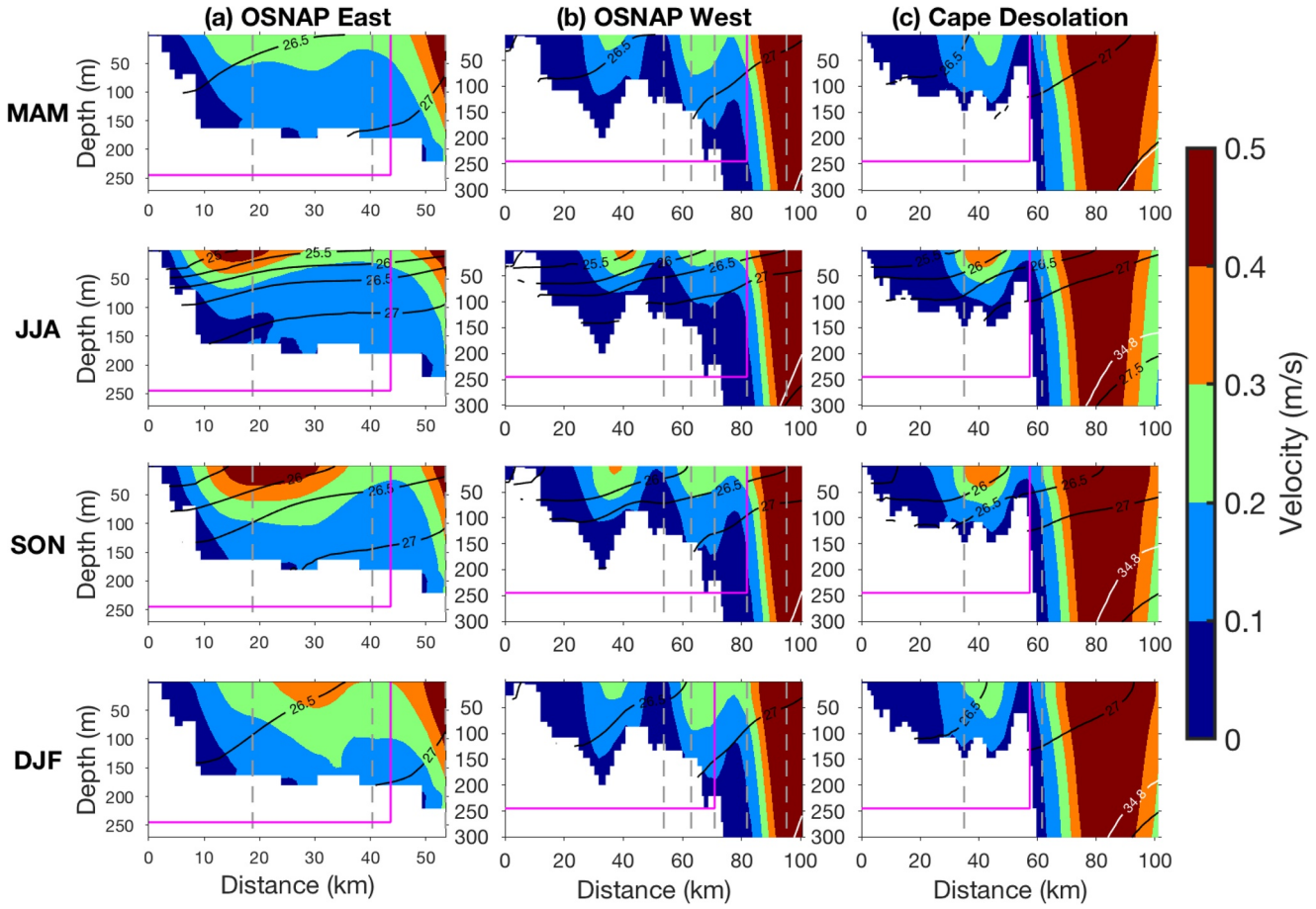

Figure 3. Seasonal velocity magnitude at Cape Desolation, OSNAP West, OSNAP East sections (a–c) averaged from 2005 to 2014 (March–May (MAM), June–August (JJA), September–November (SON) and December–February (DJF) denote boreal spring, summer, autumn and winter respectively). Pink solid lines denote the integral area for the Greenland coastal current transports. Black solid lines are isopycnals with interval equal to 0.5 kg m^{-3} and white solid lines are the 34.8 isohaline. Gray dashed lines denote the location of sectional stations. Location of the sections is shown in Figure 2. OSNAP, Overturning in the Subpolar North Atlantic Program.

Between October and March, the coastal jet merges with the main slope jet just past the Cape Farewell section. There is still a broad diffuse flow in the 0.1–0.2 m s^{-1} range northwards on the shelf at this time (Figures 2 and S4). Meanwhile, in the remaining months, a distinct current with velocities exceeding 0.2 m s^{-1} can be seen on the inner shelf.

By OSNAP West the flows have reorganized such that there are three distinct jets year round crossing this section (Figures 2a and S4). The inshore branch is strongest in summer with velocities approaching 0.4 m s^{-1}, while a second, shelf-break branch is weaker, reaching a wintertime maximum of 0.3 m s^{-1}. This splitting of the coastal flow occurs due to the presence of a small seamount just upstream of OSNAP West (Figure 2a). The third branch, along the slope, is the main WGC.

The flow gets very disorganized in Juliannehaab Bight, with at least three distinct current cores with typical upper ocean velocity ~0.2 m s^{-1} being visible on the shelf from October through March (Figure 2). The flow branching is related to bathymetric features that lead to the flow splitting and then reconnecting afterward. By AR7W, the flow has reorganized itself into a coastal current covering most of the shelf (Figures 2 and S1) plus the main slope jet. Northward, near Cape Desolation, the shelf current has narrowed and has been pushed towards the outer edge of the shelf (Figure 3). There is a more distinct band of minimum flow between the shelf and slope cores at Cape Desolation than at AR7W (Figures 2 and 3), again linked to topographic features.

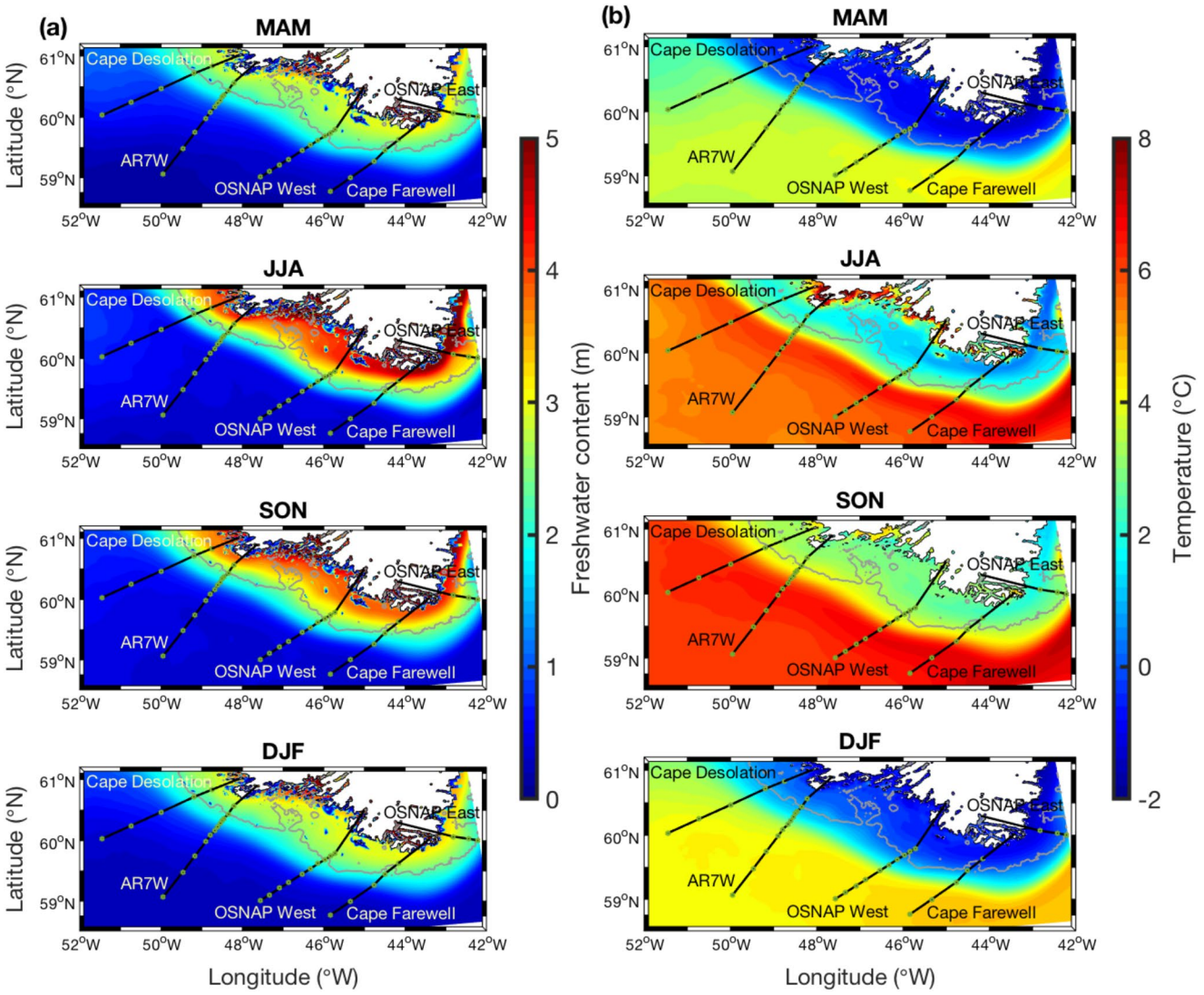

Figure 4. Horizontal maps of seasonal upper 50 m freshwater content (a) and temperature (b) averaged from 2005 to 2014 (March–May (MAM), June–August (JJA), September–November (SON) and December–February (DJF) denote boreal spring, summer, autumn and winter respectively). Location of the sections is shown in Figure 2 and gray lines denote the 250 m isobath.

The pathways of the coastal West Greenland Current system that we indicate here is very similar to that shown by the recent drifter study of Duyck and De Jong (2021). They found the coherent core of slow eddying WGCC meanders between Cape Farewell and Juliannehaab Bight. They also noticed a merging between the WGCC and WGC that is distinct compared to the clearly separated EGCC and EGC.

Seasonal upper 50 m freshwater content (reference salinity 34.8—chosen to be consistent with other studies in the region—e.g., Myers et al., 2009) and temperature distribution reveal how the water mass properties vary through the region over the year (Figure 4). This highlights the separation between water of Atlantic and polar origins and marks the transition between predominantly temperature-stratified and salinity-stratified waters (Le Bras et al., 2018), with strongest gradients of temperature and freshwater on the slope, aligned with the main current jet.

The freshwater content (Figure 4) is the highest on the continental shelf of Greenland throughout the year. This indicates that WGCC and EGCC carry fresher upper water masses than the WGC. On the continental shelf of Greenland, the freshwater content decreases from a maximum of ~4.5 m in summer to a minimum of ~3 m in winter. The summer maximum, being coastally trapped by the onshore Ekman transport during

Table 1
Annual Means (2005–2014) of Greenland Coastal Current Transports for Each Section

Section	OSNAP East	Cape Farewell	OSNAP West	AR7W	Cape Desolation
VT (Sv)	0.61	0.45	0.54	0.50	0.41
FWT (mSv)	34.4	25.8	29.4	27.1	22.0
TT(TW)	5.3	4.0	5.7	6.5	5.4

Note. VT, FWT, TT denote volume transports, freshwater transports (relative to 34.8) and heat transports (relative to −1.8°C), respectively. Freshwater and heat transports computed using other reference values are given in Table S1.

OSNAP, Overturning in the Subpolar North Atlantic Program.

this season, is likely a sign of strong Greenland melting in summer, with the fall signal consistent with the advection of meltwaters from further north off east Greenland (Benetti et al., 2019; Dukhovskoy et al., 2019).

The upper 50 m temperature (Figure 4) is not evenly distributed spatially, increasing by ∼3°C from a minimum in spring to the maximum in autumn due to seasonal surface warming. The entire shelf is close to the freezing point in winter and spring, before warming through summer. The EGCC advects colder water from the north (Figure 4), with temperatures on the shelf warming by ∼1°C–2°C from east to west.

The seasonal variability of density on the Greenland continental shelf, seen from seasonal density contours (Figures 3 and S1), is mainly driven by salinity. Therefore, the buoyancy of the upper 50 m carried by WGCC and EGCC depends on the salinity of the water (which sets the freshwater content) and thereby largely follows its seasonal variability. On the shelf, there is dense water (potential density greater than 27 kg m^{-3}) brought up each summer and fall between OSNAP East and AR7W (Figures 3 and S1), reaching the inner shelf below 150 m in June, July and August.

4. Transports of the Coastal Current System

The annual cycle of the transport in the coastal current system is presented based on the five observational sections described above. We define the transport to be positive when it is directed to the north and northwest along the main axis of the west Greenland shelf. Monthly averages are produced based on 5-daily averaged 2005–2014 model fields.

The edge of Greenland coastal current can be defined by isohaline only (34 salinity—e.g., Harden et al., 2014) or velocity only (e.g., Lin et al., 2018) or both (e.g., Sutherland et al., 2009). In the study of Foukal et al. (2020) analyzing the East Greenland boundary current system, they defined the coastal current as the inner half of the shelf and fresher than 34 salinity. Based on Foukal et al. (2020)'s definition, for all the sections indicated above except OSNAP East, we define the coastal current, and thus the transports, based on integrating the model velocity fields perpendicular to each section where the salinity is lower than 34.0 and bathymetry is shallower than 250 m (see Figure 3). As for OSNAP East, we use the position of the velocity minimum offshore of the EGCC, which we define as the 40 km mark, and also where the salinity is lower than 34.0, as the offshore edge of the coastal current. By doing so, we remove the issue of the shelf break current intruding onto the shelf at this section.

The freshwater transports and heat transports are calculated with different combinations of reference values. For the choices of different reference salinity values, previous studies use reference salinities ranging from 34.8 to 35 with different arguments (34.8 (the most common)—e.g., Lin et al., 2018 and Myers et al., 2009, 34.9—e.g., Le Bras, 2018, 35.0—e.g., Bacon et al., 2014). The freshwater transport referenced to 34.8 salinity is ∼15% larger than that to 35.0 salinity (Lin et al., 2018). As for temperature reference values, there are uses of 0°C in Myers et al. (2009) and −0.1°C in some studies focusing on the transports at Fram Strait. Therefore we choose 34.0, 34.4, 34.8, 34.9, and 35.0 as reference salinities and −1.8 (the freezing point), −0.1 and 0.0°C as reference temperatures to calculate the transports. The use of multiple reference values to compute transports provides information on the sensitivity to the choice of reference values and allows potential future studies to reconstruct the transports. Estimates referencing to 34.8 salinity and −1.8°C temperature are presented in the main manuscript (Table 1 and Figure 5), with the others in the supplementary materials (see Figures S5, S6 and Table S1).

In general, the seasonal cycle of the transports is consistent through the region, although there are some spatial differences (Figure 5). Volume transport reaches a maximum in October for all sections, and has another peak in February for all sections except for OSNAP East, where the additional peak is in January. Transport is minimum across all sections in August. The seasonal cycle in volume transport on the shelf is the largest at OSNAP East (max. ∼0.90 Sv, min. ∼0.27 Sv) to nearly flat at Cape Desolation (max. ∼0.49 Sv,

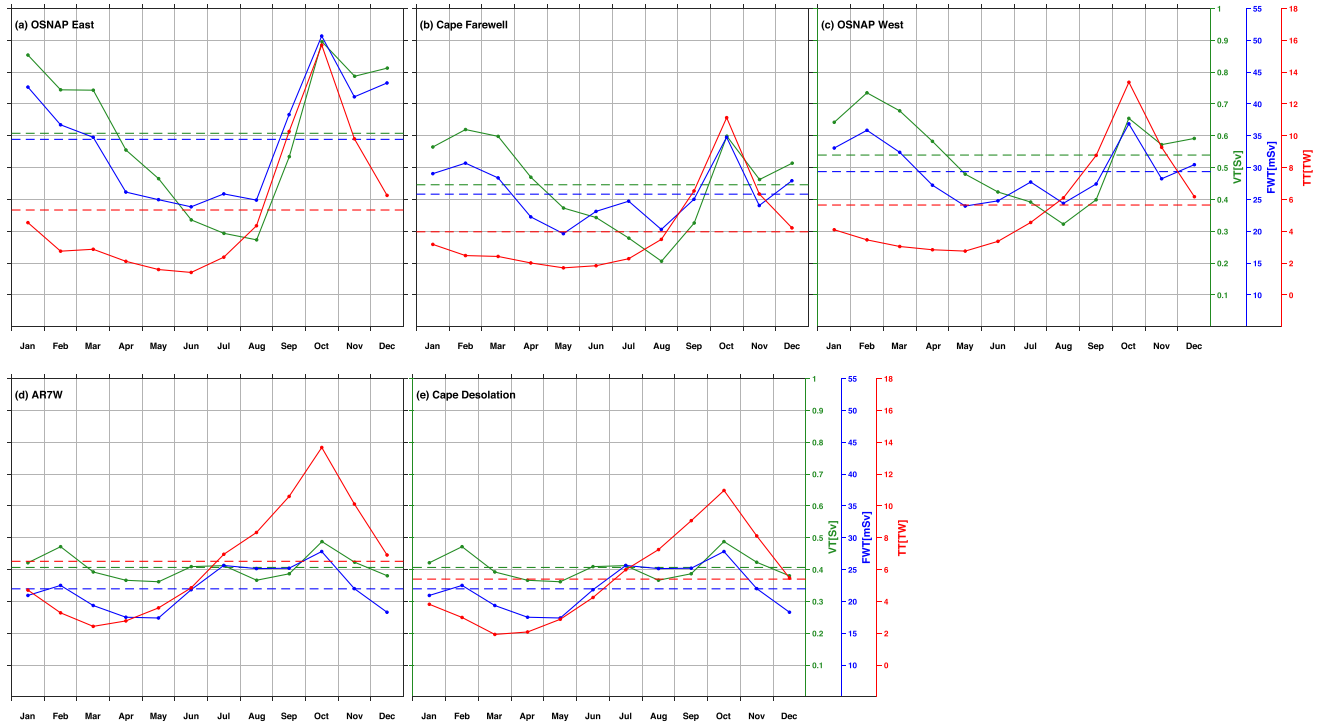

Figure 5. Mean annual cycle (2005–2014) of Greenland coastal current transports with dashed lines denoting annual means. Green, blue, red lines and y-axes correspond to volume transports, freshwater transports, heat transports respectively.

min. ~0.36 Sv). Minimum winter transport is ~0.38 Sv from Cape Desolation northwards. Comparing Figure 3a with Figure 5a, although the cross section shows much smaller current speed in the MAM time span than the JJA, the volume transport in the MAM time span is much larger than the JJA, for which we suspect the wider current core in the MAM time span is the reason. The seasonal cycle of freshwater transports closely follows the volume transports at each section. Maximum transports in October range from 50.7 mSv at OSNAP East to ~27.8 mSv at Cape Desolation. Although a minimum in freshwater transport is seen in August at OSNAP East (~24.9 mSv) and Cape Farewell (~20.3 mSv) like with the volume transport, by Cape Desolation the minimum in freshwater transport occurs in April and May (~17.5 mSv). Heat transport also has an October maximum (~15.7 TW at OSNAP East through to ~11.0 TW at Cape Desolation). However, the heat transport is generally low through winter when the shelf waters are cold, leading to minimum transports of ~2–4 TW through winter and early spring.

As well as a reduction in the amplitude of the seasonal cycle as one moves north and west along the shelf, there is also a reduction in the net transports. From a net transport on the shelf of ~0.61 Sv at OSNAP East, there is a reduction to ~0.50 Sv at AR7W. Although our annual averaged transport estimated at Cape Farewell is only ~0.45 Sv, this may be an underestimate due to the narrowness of the shelf and the fact that positive velocities can be seen in deeper water that are well distinct from the main slope current (Figure 3). A significant reduction of ~0.09 Sv in the net shelf transport occurs over the short distance between AR7W and Cape Desolation. Similar reductions are seen in the freshwater transport, from a long term mean of ~34.4 mSv at OSNAP East to ~29.4 mSv at OSNAP West, and then another drop of ~5.1 mSv from AR7W to Cape Desolation. Net heat transport doesn't vary much, remaining about ~6 TW across all sections (other than Cape Farewell, which is likely underestimated as discussed above).

5. Discussion, Conclusions and Perspectives

Using a very high-resolution (1°/60°) numerical simulation from 2005 to 2014, the annual cycle of the current structure in the vicinity of southern Greenland is analyzed to present the seasonal variability of West Greenland Current System, including the WGCC. We also examine the model transports on the shelf to reveal the seasonal variability in a more quantitative perspective.

At OSNAP East, our results are consistent with Le Bras et al. (2018) in that the EGCC is a distinct core inshore of the shelf-break EGC. We also find winter intensified freshwater transport in the EGCC. Our transport maximum in October is similar to that seen by Le Bras et al. (2018) for 2015, but earlier by 1–2 months compared to 2014, suggesting the presence of significant inter-annual variability. We find that a shelf break WGCC exists for about half the year between Cape Farewell and Cape Desolation. Near Cape Farewell, the coastal flow merges with the main WGC in winter and separates from the shelf break current between April and September.

The separation of the two currents in the model summer coincides with the analysis of cruise data around Cape Farewell in summer 2014 (Lin et al., 2018), indicating that the EGCC continues as a coastal current (WGCC) after encountering Cape Farewell rather than merging to form WGC. Additionally, this part of the coastal current still connects to the shelf break current in May to the extent that a broad diffuse flow exists in between, with a clear separation starting in June (Figure 2). This is consistent for the transition from inexistence in May 2014 to existence in June 2014 of the WGCC in a cruise study (Benetti et al., 2019).

There is a three current system when the shelf widens in Juliannehaab Bight: A shelf component, a shelf-break component and a main slope jet. A two-branch pattern of WGCC bifurcation in this region was revealed by Lin et al. (2018), with a main branch on the outer shelf and a minor branch on the inner shelf. We show that this feature occurs due to a small seamount just upstream of OSNAP West, where the bottom rises from a background depth of ~150 m to a minimum depth of 11 m.

As the shelf narrows at Cape Desolation, the flow reorganizes into the coastal current and the main slope jet without a shelf-break current. A single deep velocity core at Cape Desolation, reaching down into the Irminger Water at depth, is consistent with Fratantoni and Pickart (2007). Neither Myers et al. (2009) nor Rykova et al. (2015) were able to resolve the coastal shelf current from the hydrographic data they used although lowered acoustic Doppler current profiler data presented by Hall et al. (2013) in their Figure 2b hints at a distinct flow on the shelf at AR7W.

The previous paper that presents the model configuration (Pennelly & Myers, 2020) included as part of its supplementary material a video showing the evolution of the model mixed layer in the Labrador Sea. That video (https://doi.org/10.7939/r3-m6rk-h867) also shows the model sea ice edge (10% concentration). In the simulation, sea ice covers the EGCC area basically from January to May. But for the most part, the sea ice does not penetrate past Cape Farewell to cover the WGCC area along the shelf. Some ice is produced locally but does not seem to grow/migrate away. However, known years with strong convection/cold winters (e.g., 2008, 2009, and 2012) have most of the shelf west of Greenland covered in sea ice in February and March. Satellite observation also shows that during the sea ice maximum in April and May, the sea ice may cover the EGCC but does not penetrate into the WGCC area at all (Le Bras et al., 2018). The sea-ice concentration is generally low enough that it is likely to have little impact on the circulation in the region, although we do show slowest coastal current speed in May (Figure 2), which is potentially due to the impact of the sea ice on the EGCC.

Our long term shelf transport at OSNAP East of 0.61 Sv is smaller than Le Bras et al. (2018)'s 0.86 ± 0.1 Sv, but our freshwater transport of 36.1 mSv (relative to 34.9) is close to their 42 ± 6 mSv (relative to 34.9). Furthermore, our seasonal range of 25–50 mSv is also close to that of Le Bras et al. (2018) in both magnitude and phase. The difference between our transports and Le Bras et al. (2018)'s transports could be due to the short timespan of the OSNAP East data they used, which is only 24-month and for a period that began several years after the end of our model analysis period. For example, using a configuration functionally equivalent to the outer nest used here, Pennelly and Myers (2021) computed the freshwater transport in the EGC at Cape Farewell. Although they used a slightly different definition of shelf water ($S < 34.8$, $\sigma_\theta < 1{,}027.68$ kg m^{-3}),

and used multiple wind stress forcing products, their timeseries showed larger transports over 2014–2016 compared to our averaging period of 2005–2014 here.

Our estimates for along shelf transport at Cape Farewell and OSNAP West are smaller than those observed by Lin et al. (2018) for their k5 and k7 sections. As stated above, our Cape Farewell estimates are likely low because of how we chose to define the coastal current. The reason is less clear for OSNAP West, especially as August is our month for minimum coastal current transport. That said, there is significant inter-annual variability, and Lin et al. (2018)'s 2014 measurements are from a year that Pennelly et al. (2019) find has strong alongshore freshwater transport of Polar Water at Cape Desolation.

Rykova et al. (2015) used 18 occupations of AR7W (five in winter) and altimeter-derived surface velocity to reconstruct the boundary current system at AR7W. Meanwhile Myers et al. (2009) used summer hydrographic data and a frontal model to examine the WGC at Cape Desolation. Our transport numbers for AR7W through to Cape Desolation of 0.4–0.5 Sv and 22–27 mSv are not directly comparable with either Myers et al. (2009) or Rykova et al. (2015) since they both focused on the WGC and had little resolution on the shelf. Although Myers et al. (2009) estimated a larger transport for the non-Irminger Water portion of the WGC of 3.7 Sv using their frontal model, Rykova et al. (2015) found 2.0 Sv using a different definition of the Irminger Water boundary. Still, in either case, even though the shelf has narrowed significantly by Cape Desolation, a WGCC transport of 0.4 Sv is not negligible. More significant is that our annually averaged shelf freshwater transport estimates are around a third of the 55–60 mSv WGC transport found at similar locations by Myers et al. (2009) and Rykova et al. (2015).

The net transport of the coastal current system decreases northward and westward along the shelf. In our model, the 25% decrease of the freshwater transports from 34.4 mSv at OSNAP East to 25.8 mSv at Cape Farewell is basically consistent with the observed freshwater transport loss of the coastal current as it rounds Cape Farewell (29%, Lin et al., 2018). This decrease in transport is most likely the results of substantial exchange of WGCC water with WGC (Lin et al., 2018), transporting its cold, fresh Upper Polar Water (UPW, Pacini et al., 2020) into the WGC. However, our Cape Farewell estimates are likely low because of how we chose to define the coastal current. Thus, it may be that more freshwater leaves the coastal current along the west Greenland shelf after Cape Farewell than before it along the east Greenland shelf. Yet Duyck and De Jong (2021) found drifters, and thus freshwater, exchanged between coastal flows and the shelfbreak, on both sides of Cape Farewell.

Given that the main EGC/WGC system at Cape Farewell transports 11.7 Sv after losing water to a retroflection (Holliday et al., 2007), the coastal current is not a significant source of water to the main current system. However, given annual averaged estimates of EGC freshwater transport of 42 mSv at OSNAP East (Le Bras et al., 2018) and 55–60 mSv at AR7W/Cape Desolation (Myers et al., 2009; Rykova et al., 2015), this export from the coastal system explains the increase seen in the main WGC freshwater transport in this region. Although the estimates of Myers et al. (2009) and Rykova et al. (2015) may include some of the coastal current transport, unless all of the freshwater on the shelf remains there through to Davis Strait, then the net export of freshwater from the WGC system to the Labrador Sea interior is likely to be in the 75–80 mSv range, which is larger than previously thought. Additionally, given the exchange of freshwater from the coastal current to the boundary current as the flow rounds Cape Farewell, any additional meltwater from a warming East Greenland is likely to end up in the Labrador Sea. Yet, the 22 mSv of freshwater transport remaining on the shelf at Cape Desolation suggests that some of this offshore exchange of low salinity water occurs farther north in the Labrador Sea and may not be directly impacting the deep convection site, instead playing a role in increasing the stratification in the northern Labrador Sea (Chanut et al., 2008; Luo et al., 2016; Pennelly & Myers, 2020; Tagklis et al., 2020). The coastal current will also receive a contribution from Greenland melt to West Greenland as it flows north, although much of this water is likely to remain near the coast and enter Baffin Bay (Gillard et al., 2016). That said, the behavior of the WGC in the northern Labrador Sea is under-studied and worth further examination.

Conflict of Interest

The authors declare no conflicts of interest relevant to this study.

Data Availability Statement

The Fortran code used to carry out the LAB60 simulation can be accessed from the NEMO version 3.6 repository (https://forge.ipsl.jussieu.fr/nemo/browser/NEMO/releases/release-3.6, last access: October 14, 2020). A few Fortran files were modified to handle our passive tracers. The complete Fortran files as well as the CPP keys, namelists, and associated files can be found on Zenodo (https://doi.org/10.5281/zenodo.3762748, Pennelly, 2020). The initial and boundary conditions, atmospheric forcing, and numerical output were too large to host on a repository and are instead hosted on our lab's servers as well as the Compute Canada Niagara (http://www.computecanada.ca). OSNAP data were collected and made freely available by the OSNAP (Overturning in the Subpolar North Atlantic Program) project and all the national programs that contribute to it (www.o-snap.org).

Acknowledgments
This work was funded by Natural Sciences and Engineering Research Council of Canada (NSERC) grants awarded to PGM. These include Discovery Grants (rgpin 227438-09 and 2020-04344) and a Climate Change and Atmospheric Research Grant (433898). GLORYS reanalysis received support from Mercator Ocean, Groupe Mission Mercator Coriolis and the European Communitys Seventh Framework Program FP7/2007-2013 under Grant Agreement number 218812 (MyOcean). The authors would like to thank the NEMO development team as well as the DRAKKAR group for providing the model code and continuous guidance. Ruijian Gou's internship at the University of Alberta was funded by the China Scholarship Council.

References

Aagaard, K., & Carmack, E. C. (1989). The role of sea ice and other fresh water in the Arctic circulation. *Journal of Geophysical Research*, *94*(C10), 14485–14498. https://doi.org/10.1029/JC094iC10p14485

Amante, C., & Eakins, B. W. (2009). ETOPO1 1 Arc-minute global relief model: Procedures data sources and analysis. NOAA Technical Memorandum NESDIS. NGDC-24 19.

Bacon, S., Marshall, A., Holliday, N. P., Aksenov, Y., & Dye, S. R. (2014). Seasonal variability of the east Greenland coastal current. *Journal of Geophysical Research: Oceans*, *119*(6), 3967–3987. https://doi.org/10.1002/2013JC009279

Bacon, S., Reverdin, G., Rigor, I. G., & Snaith, H. M. (2002). A freshwater jet on the east Greenland shelf. *Journal of Geophysical Research*, *107*(C7), 3068. https://doi.org/10.1029/2001JC000935

Bamber, J., van den Broeke, M., Ettema, J., Lenaerts, J., & Rignot, E. (2012). Recent large increases in freshwater fluxes from Greenland into the North Atlantic. *Geophysical Research Letters*, *39*(19), L19501. https://doi.org/10.1029/2012GL052552

Barnier, B., Brodeau, L., le Sommer, J. M., Molines, T., Penduff, S., Theetten, A. M., et al. (2007). Eddy-permitting ocean circulation hindcasts of past decades. *Clivar Exchanges*, *42*(12(3)), 8–10.

Benetti, M., Reverdin, G., Clarke, J. S., Tynan, E., Holliday, N. P., Torres-Valdes, S., et al. (2019). Sources and distribution of fresh water around Cape Farewell in 2014. *Journal of Geophysical Research: Oceans*, *124*(12), 9404–9416. https://doi.org/10.1029/2019JC015080

Bracco, A., Pedlosky, J., & Pickart, R. S. (2008). Eddy formation near the west coast of Greenland. *Journal of Physical Oceanography*, *38*(9), 1992–2002. https://doi.org/10.1175/2008JPO3669.1

Chanut, J., Barnier, B., Large, W., Debreu, L., Penduff, T., Molines, J. M., & Mathiot, P. (2008). Mesoscale eddies in the Labrador Sea and their contribution to convection and restratification. *Journal of Physical Oceanography*, *38*(8), 1617–1643. https://doi.org/10.1175/2008jpo3485.1

Cuny, J., Rhines, P. B., Niiler, P. P., & Bacon, S. (2002). Labrador Sea boundary currents and the fate of the Irminger Sea water. *Journal of Physical Oceanography*, *32*(2), 627–647. https://doi.org/10.1175/1520-0485(2002)032<0627:lsbcat>2.0.co;2

Dai, A., Qian, T., Trenberth, K. E., & Milliman, J. D. (2009). Changes in continental freshwater discharge from 1948 to 2004. *Journal of Climate*, *22*(10), 2773–2792. https://doi.org/10.1175/2008JCLI2592.1

Dai, A., & Trenberth, K. E. (2002). Estimates of freshwater discharge from continents: Latitudinal and seasonal variations. *Journal of Hydrometeorology*, *3*(6), 660–687. https://doi.org/10.1175/1525-7541(2002)003<0660:EOFDFC>2.0.CO;2

Danabasoglu, G., Yeager, S. G., Kim, W. M., Behrens, E., Bentsen, M., Bi, D., et al. (2016). North Atlantic simulations in coordinated ocean-ice reference experiments phase II (CORE-II). Part II: Inter-annual to decadal variability. *Ocean Modelling*, *97*, 65–90. https://doi.org/10.1016/j.ocemod.2015.11.007

Debreu, L., Vouland, C., & Blayo, E. (2008). AGRIF: Adaptive grid refinement in Fortran. *Computers & Geosciences*, *34*(1), 8–13. https://doi.org/10.1016/j.cageo.2007.01.009

de Jong, M. F., Bower, A. S., & Furey, H. H. (2014). Two years of observations of warm-core anticyclones in the Labrador Sea and their seasonal cycle in heat and salt stratification. *Journal of Physical Oceanography*, *44*(2), 427–444. https://doi.org/10.1175/JPO-D-13-070.1

Dukhovskoy, D. S., Yashayaev, I., Proshutinsky, A., Bamber, J. L., Bashmachnikov, I. L., Chassignet, E. P., et al. (2019). Role of Greenland freshwater anomaly in the recent freshening of the subpolar North Atlantic. *Journal of Geophysical Research: Oceans*, *124*(5), 3333–3360. https://doi.org/10.1029/2018JC014686

Duyck, E., & De Jong, M. F. (2021). Circulation over the South-East Greenland shelf and potential for liquid freshwater export: A drifter study. *Geophysical Research Letters*, *48*, e2020JB020886. https://doi.org/10.1029/2020GL091948

Ferry, N., Parent, L., Garric, G., Barnier, B., & Jourdain, N. C. (2010). Mercator global eddy permitting ocean reanalysis GLORYS1V1: Description and results. *Mercator-Ocean Quarterly Newsletter*, *36*, 15–27.

Feucher, C., Garcia-Quintana, Y., Yashayaev, I., Hu, X., & Myers, P. G. (2019). Labrador Sea water formation rate and its impact on the local meridional overturning circulation. *Journal of Geophysical Research: Oceans*, *124*(8), 5654–5670. https://doi.org/10.1029/2019JC015065

Foukal, N. P., Gelderloos, R., & Pickart, R. S. (2020). A continuous pathway for fresh water along the East Greenland shelf. *Science Advances*, *6*(43), eabc4254. https://doi.org/10.1126/sciadv.abc4254

Fratantoni, D. M. (2001). North Atlantic surface circulation during the 1990's observed with satellite-tracked drifters. *Journal of Geophysical Research*, *106*(C10), 22067–22093. https://doi.org/10.1029/2000JC000730

Fratantoni, P. S., & Pickart, R. S. (2007). The Western North Atlantic shelfbreak current system in summer. *Journal of Physical Oceanography*, *37*(10), 2509–2533. https://doi.org/10.1175/JPO3123.1

Gillard, L. C., Hu, X., Myers, P. G., & Bamber, J. L. (2016). Meltwater pathways from marine terminating glaciers of the Greenland ice sheet. *Geophysical Research Letters*, *43*(20), 10873–10882. https://doi.org/10.1002/2016GL070969

Haine, T. W. N., Curry, B., Gerdes, R., Hansen, E., Karcher, M., Lee, C., et al. (2015). Arctic freshwater export: Status, mechanisms, and prospects. *Global and Planetary Change*, *125*, 13–35. https://doi.org/10.1016/j.gloplacha.2014.11.013

Hall, M. M., Torres, D. J., & Yashayaev, I. (2013). Absolute velocity along the AR7W section in the Labrador Sea. *Deep Sea Research Part I: Oceanographic Research Papers*, *72*, 72–87. https://doi.org/10.1016/j.dsr.2012.11.005

Harden, B. E., Pickart, R. S., & Renfrew, I. A. (2014). Offshore transport of dense water from the East Greenland shelf. *Journal of Physical Oceanography*, *44*(1), 229–245. https://doi.org/10.1175/JPO-D-12-0218.1

Holliday, N. P., Meyer, A., Bacon, S., Alderson, S. G., & De Cuevas, B. (2007). Retroflection of part of the east Greenland current at Cape Farewell. *Geophysical Research Letters*, *34*(7), L07609. https://doi.org/10.1029/2006GL029085

Hu, X., Sun, J., Chan, T. O., & Myers, P. G. (2018). Thermodynamic and dynamic ice thickness contributions in the Canadian Arctic Archipelago in NEMO-LIM2 numerical simulations. *The Cryosphere*, *12*(4), 1233–1247. https://doi.org/10.5194/tc-12-1233-2018

IPCC (2013). Summary for Policymakers. In T. F. Stocker, D. Qin, G.-K. Plattner, M. Tignor, S. K. Allen, J. Boschung, et al. (Eds.), *Climate change 2013: The physical science basis. Contribution of working group I to the fifth assessment report of the Intergovernmental panel on climate change*. Cambridge and New York, NY: Cambridge University Press.

Katsman, C. A., Spall, M. A., & Pickart, R. S. (2004). Boundary current eddies and their role in the restratification of the Labrador Sea. *Journal of Physical Oceanography*, *34*(9), 1967–1983. https://doi.org/10.1175/1520-0485(2004)034<1967:bceatr>2.0.co;2

Le Bras, I. A. A., Straneo, F., Holte, J., & Holliday, N. P. (2018). Seasonality of freshwater in the east Greenland current system from 2014 to 2016. *Journal of Geophysical Research: Oceans*, *123*(12), 8828–8848. https://doi.org/10.1029/2018JC014511

Lilly, J. M., Rhines, P. B., Schott, F., Lavender, K., Lazier, J., Send, U., & D'Asaro, E. (2003). Observations of the Labrador Sea eddy field. *Progress in Oceanography*, *59*(1), 75–176. https://doi.org/10.1016/j.pocean.2003.08.013

Lin, P., Pickart, R. S., Torres, D. J., & Pacini, A. (2018). Evolution of the freshwater coastal current at the Southern tip of Greenland. *Journal of Physical Oceanography*, *48*(9), 2127–2140. https://doi.org/10.1175/JPO-D-18-0035.1

Lozier, M. S., Bacon, S., Bower, A. S., Cunningham, S. A., de Jong, M. F., de Steur, L., et al. (2017). Overturning in the subpolar north Atlantic program: A new international ocean observing system. *Bulletin of the American Meteorological Society*, *98*, 737–752. https://doi.org/10.1175/BAMS-D-16-0057.1

Lozier, M. S., Li, F., Bacon, S., Bahr, F., Bower, A. S., Cunningham, S. A., et al. (2019). A sea change in our view of overturning in the subpolar North Atlantic. *Science*, *363*(6426), 516–521. https://doi.org/10.1126/science.aau6592

Luo, H., Castelao, R. M., Rennermalm, A. K., Tedesco, M., Bracco, A., Yager, P. L., & Mote, T. L. (2016). Oceanic transport of surface meltwater from the southern Greenland ice sheet. *Nature Geoscience*, *9*(7), 528–532. https://doi.org/10.1038/ngeo2708

Madec, G. (2008). *Nemo ocean engine, Note du Pôle de modélisation, 27*. Institut Pierre-Simon Laplace (IPSL).

Marson, J. M., Myers, P. G., Hu, X., & Le Sommer, J. (2018). Using vertically integrated ocean fields to characterize Greenland icebergs' distribution and lifetime. *Geophysical Research Letters*, *45*, 4208–4217. https://doi.org/10.1029/2018GL077676

Mortensen, J. (2018). *Report on hydrographic conditions off Southwest Greenland June/July 2017*. NAFO SCR Doc 18/005, Serial No. N6782.

Myers, P. G. (2005). Impact of freshwater from the Canadian Arctic archipelago on Labrador Sea water formation. *Geophysical Research Letters*, *32*(6), L06605. https://doi.org/10.1029/2004GL022082

Myers, P. G., & Donnelly, C. (2008). Water mass transformation and formation in the Labrador Sea. *Journal of Climate*, *21*(7), 1622–1638. https://doi.org/10.1175/2007JCLI1722.1

Myers, P. G., Donnelly, C., & Ribergaard, M. H. (2009). Structure and variability of the west Greenland current in summer derived from 6 repeat standard sections. *Progress in Oceanography*, *80*(1–2), 93–112. https://doi.org/10.1016/j.pocean.2008.12.003

Myers, P. G., Kulan, N., & Ribergaard, M. H. (2007). Irminger Water variability in the west Greenland current. *Geophysical Research Letters*, *34*(17), 217–239. https://doi.org/10.1029/2007GL030419

Pacini, A., Pickart, R. S., Bahr, F., Torres, D. J., Ramsey, A. L., Holte, J., et al. (2020). Mean conditions and seasonality of the west Greenland boundary current system near Cape Farewell. *Journal of Physical Oceanography*, *50*(10), 2849–2871. https://doi.org/10.1175/JPO-D-20-0086.1

Pennelly, C., Hu, X., & Myers, P. G. (2019). Cross-Isobath freshwater exchange within the north Atlantic subpolar gyre. *Journal of Geophysical Research: Oceans*, *124*(10), 6831–6853. https://doi.org/10.1029/2019JC015144

Pennelly, C., & Myers, P. G. (2020). Introducing LAB60: A 1/60° NEMO 3.6 numerical simulation of the Labrador Sea. *Geoscientific Model Development*, *13*, 4959–4975. https://doi.org/10.5194/gmd-2020-111

Pennelly, C., & Myers, P. G. (2021). Impact of different atmospheric forcing sets on modeling Labrador Sea Water production. *Journal of Geophysical Research: Oceans*, *126*(2), e2020JC016452. https://doi.org/10.1029/2020JC016452

Rykova, T., Straneo, F., & Bower, A. S. (2015). Seasonal and interannual variability of the west Greenland current system in the Labrador Sea in 1993–2008. *Journal of Geophysical Research: Oceans*, *120*(2), 1318–1332. https://doi.org/10.1002/2014jc010386

Schmidt, S., & Send, U. (2007). Origin and composition of seasonal Labrador Sea freshwater. *Journal of Physical Oceanography*, *37*(6), 1445–1454. https://doi.org/10.1175/JPO3065.1

Schulze-Chretien, L. M., & Frajka-Williams, E. (2018). Wind-driven transport of fresh shelf water into the upper 30 m of the Labrador Sea. *Ocean Science*, *14*(5), 1247–1264. https://doi.org/10.5194/os-14-1247-2018

Smith, G. C., Roy, F., Mann, P., Dupont, F., Brasnett, B., Lemieux, J.-F., et al. (2014). A new atmospheric dataset for forcing ice-ocean models: Evaluation of reforecasts using the Canadian global deterministic prediction system. *Quarterly Journal of the Royal Meteorological Society*, *140*(680), 881–894. https://doi.org/10.1002/qj.2194

Stouffer, R. J., Seidov, D., & Haupt, B. J. (2007). Climate response to external sources of freshwater: North Atlantic versus the Southern Ocean. *Journal of Climate*, *20*(3), 436–448. https://doi.org/10.1175/JCLI4015.1

Straneo, F. (2006). Heat and freshwater transport through the central Labrador Sea. *Journal of Physical Oceanography*, *36*(4), 606–628. https://doi.org/10.1175/JPO2875.1

Sutherland, D. A., & Pickart, R. S. (2008). The east Greenland coastal current: Structure, variability, and forcing. *Progress in Oceanography*, *78*(1), 58–77. https://doi.org/10.1016/j.pocean.2007.09.006

Sutherland, D. A., Pickart, R. S., Peter Jones, E., Azetsu-Scott, K., Jane Eert, A., & Ólafsson, J. (2009). Freshwater composition of the waters off southeast Greenland and their link to the Arctic Ocean. *Journal of Geophysical Research*, *114*(C5), C05020. https://doi.org/10.1029/2008JC004808

Tagklis, F., Bracco, A., Ito, T., & Castelao, R. M. (2020). Submesoscale modulation of deep water formation in the Labrador Sea. *Scientific Reports*, *10*, 17489. https://doi.org/10.1038/s41598-020-74345-w

Tsujino, H., Urakawa, S., Nakano, H., Small, R. J., Kim, W. M., Yeager, S. G., et al. (2018). JRA-55 based surface dataset for driving ocean-sea-ice models (JRA55-do). *Ocean Modelling*, *130*, 79–139. https://doi.org/10.1016/j.ocemod.2018.07.002

Vellinga, M., & Wood, R. A. (2002). Global climatic impacts of a collapse of the Atlantic thermohaline circulation. *Climatic Change*, *54*, 251–267. https://doi.org/10.1023/A:1016168827653

Weijer, W., Maltrud, M. E., Hecht, M. W., Dijkstra, H. A., & Kliphuis, M. A. (2012). Response of the Atlantic Ocean circulation to Greenland ice sheet melting in a strongly-eddying ocean model. *Geophysical Research Letters*, *39*(9), L09606. https://doi.org/10.1029/2012GL051611

White, M. A., & Heywood, K. J. (1995). Seasonal and interannual changes in the North Atlantic subpolar gyre from Geosat and TOPEX/Poseidon altimetry. *Journal of Geophysical Research*, *100*(C12), 24931–24941. https://doi.org/10.1029/95jc02123

Wilkinson, D., & Bacon, S. (2005). The spatial and temporal variability of the east Greenland coastal current from historic data. *Geophysical Research Letters*, *32*(24), L24618. https://doi.org/10.1029/2005GL024232

Yang, Q., Dixon, T. H., Myers, P. G., Bonin, J., Chambers, D., van den Broeke, M. R., et al. (2016). Recent increases in Arctic freshwater flux affects Labrador Sea convection and Atlantic overturning circulation. *Nature Communications*, *7*, 10525. https://doi.org/10.1038/ncomms10525

Yashayaev, I., & Loder, J. W. (2017), Further intensification of deep convection in the Labrador Sea in 2016. *Geophysical Research Letters*, *44*, 1429–1438. https://doi.org/10.1002/2016GL071668